

## Article

# Transcriptome Analysis of Cambium Tissue of Paulownia Collected during Winter and Spring

Zachary D. Perry<sup>1</sup>, Thangasamy Saminathan<sup>2</sup>, Alok Arun<sup>3</sup> , Brajesh N. Vaidya<sup>1</sup>, Chhandak Basu<sup>4</sup>, Umesh K. Reddy<sup>2</sup>  and Nirmal Joshee<sup>1,\*</sup> 

<sup>1</sup> Agricultural Research Station, Fort Valley State University, Fort Valley, GA 31030, USA; Zachary.Perry@usda.gov (Z.D.P.); braz\_v@hotmail.com (B.N.V.)

<sup>2</sup> Gus R. Douglass Institute and Department of Biology, West Virginia State University, Institute, WV 25112, USA; tsaminathan@wvstate.edu (T.S.); uredy@wvstateu.edu (U.K.R.)

<sup>3</sup> Institute of Sustainable Biotechnology, Inter American University of Puerto Rico, Barranquitas, PR 00794, USA; alok\_arun@br.inter.edu

<sup>4</sup> Department of Biology, California State University, Northridge, Los Angeles, CA 91330, USA; chhandak.basu@csun.edu

\* Correspondence: josheen@fvsu.edu

**Abstract:** Paulownia (*Paulownia elongata*) is a fast-growing, multipurpose deciduous hardwood species that grows in a wide range of temperatures from  $-30^{\circ}\text{C}$  to  $45^{\circ}\text{C}$ . Seasonal cues influence the secondary growth of tree stems, including cambial activity, wood chemistry, and transition to latewood formation. In this study, a de novo transcriptome approach was conducted to identify the transcripts expressed in vascular cambial tissue from senescent winter and actively growing spring seasons. An Illumina paired-end sequenced cambial transcriptome generated 297,049,842 clean reads, which finally yielded 61,639 annotated unigenes. Based on non-redundant protein database analyses, Paulownia cambial unigenes shared the highest homology (64.8%) with *Erythranthe guttata*. KEGG annotation of 35,471 unigenes identified pathways enriched in metabolic activities. Transcriptome-wide DEG analysis showed that 2688 and 7411 genes were upregulated and downregulated, respectively, in spring tissues compared to winter. Interestingly, several transcripts encoding heat shock proteins were upregulated in the spring season. RT-qPCR expression results of fifteen wood-forming candidate genes involved in hemicellulose, cellulose, lignin, auxin, and cytokinin pathways showed that the hemicellulose genes (*CSLC4*, *FUT1*, *AXY4*, *GATL1*, and *IRX19*) were significantly upregulated in spring season tissues when compared to winter tissues. In contrast, lignin pathway genes *CCR1* and *CAD1* were upregulated in winter cambium. Finally, a transcriptome-wide marker analysis identified 11,338 Simple Sequence Repeat (SSRs). The AG/CT dinucleotide repeat predominately represented all SSRs. Altogether, the cambial transcriptomic analysis reported here highlights the molecular events of wood formation during winter and spring. The identification of candidate genes involved in the cambial growth provides a roadmap of wood formation in Paulownia and other trees for the seasonal growth variation.

**Keywords:** Paulownia; cambium; transcriptome; winter season; spring season; tree growth



**Citation:** Perry, Z.D.; Saminathan, T.; Arun, A.; Vaidya, B.N.; Basu, C.; Reddy, U.K.; Joshee, N. Transcriptome Analysis of Cambium Tissue of Paulownia Collected during Winter and Spring. *Diversity* **2021**, *13*, 423. <https://doi.org/10.3390/d13090423>

Academic Editor: Michael Wink

Received: 14 July 2021

Accepted: 27 August 2021

Published: 1 September 2021

**Publisher's Note:** MDPI stays neutral with regard to jurisdictional claims in published maps and institutional affiliations.



**Copyright:** © 2021 by the authors. Licensee MDPI, Basel, Switzerland. This article is an open access article distributed under the terms and conditions of the Creative Commons Attribution (CC BY) license (<https://creativecommons.org/licenses/by/4.0/>).

## 1. Introduction

Paulownia (*Paulownia elongata*) is an extremely fast-growing woody plant growing up to 20 feet in one year when young. Some *Paulownia* spp., when in plantation, can be harvested for saw timber in as little as five years. The genus *Paulownia* consists of nine species of deciduous, fast-growing, multi-purpose, hardwood trees [1] that have long been shown to be extremely adaptive to wide environmental variations in both edaphic and climatic factors, as well as being capable of growing on marginal lands [2,3]. Species of *Paulownia* are native to Asia and are widely cultivated in China, Laos, Vietnam, Japan, and Korea. It has now been introduced and cultivated in Australia, Europe, and

North and Central America. Ten-year-old Paulownia trees, in natural conditions, can attain 30–40 cm in diameter at breast height (DBH) and a timber volume of 0.3–0.5 m<sup>3</sup> [1]. Craftworkers in Japan and other countries have used this valuable wood to create intricate carvings, surfboards, musical instruments, toys, and furniture. Paulownia wood has a high ignition point of 420–430 °C compared to other hardwoods, which generally range from 220–225 °C, thus making Paulownia wood fire retardant [4,5]. Paulownia plants bear abundant flowers that are highly nectariferous and yield premium honey [6], adding to the rural economy. By adding Paulownia wood flour (25–40%) to plastics, an attractive, equally strong, environmentally agreeable, and economically important biocomposite can be produced [7–9] to serve many industries. Additionally, the lightweight and strong nature of the wood makes it widely applicable in the music industry for preparing the finer components of instruments. Biochar produced from Paulownia is also a desirable organic soil amendment that allows the growth of beneficial microbes in the porous holes of the biochar [10]. Recently, researchers found its potential use as an animal feed resource [11].

Wood synthesis provides one of the most important sinks for atmospheric carbon dioxide [12]. Wood formation is a result of the regulated accumulation of secondary xylem cells (fibers, vessels, and rays in dicots) differentiated from the vascular cambium that involves wall thickening. This wall thickening is accompanied by the biosynthesis of wall components, lignin, cellulose, and hemicelluloses and is terminated by programmed cell death [13,14]. In order to survive multiple growing seasons, perennial plant species have adapted a dormancy regulation system that allows active growth during the desirable time of year and vegetative dormancy when climatic conditions are unfavorable for growth [15]. The Paulownia tree, due to its fast-growing nature, is capable of producing ~45 kg/tree in the first growing year and ~90 kg/tree at the end of the second year [16]. Being a perennial tree, Paulownia harvest is not limited to a small seasonal window but can be conducted year-round with proper management practices. Another beneficial property of Paulownia is coppicing, which is defined as the production of multiple sprouts from a stump after the removal of the tree or shrub. Harvest cycles of 2–3 years could be implemented to establish a fast-growing bioenergy crop. Since Paulownia is a short-rotation fast-growing perennial tree and serves as a good candidate to produce lignocellulosic biofuel, which can eliminate dependence on fossil fuel.

Transcriptome analyses from various tree species indicate that the putative role of gene families belonging to receptor kinases, transcription factors, and secondary wall biosynthesis are highly expressed in wood-forming cells [17–21]. At a molecular level, studies related to Paulownia gene expression profiling published in the last few years have primarily focused on drought tolerance and host-pathogen interactions [22–25]. Cambial development (the initiation and activity of the vascular cambium) leads to an accumulation of wood (secondary xylem tissue). Seasonal cues play a significant role in determining cambial growth as perennial plants growing in temperate and high-latitude regions show termination of cell division in the meristems [26] and reversal of growth arrest during long days [27]. Time-coursed RNA sequence studies identified downregulated phytohormone-related genes (IAA, ARF, and SAURs) and upregulated circadian genes (PIF3 and PRR5; [28,29]. A transcriptome-wide profiling study in *P. elongata* identified a subset of candidate genes that contribute to the production of wood [30] by investigating the differential expression of transcripts of the vascular cambium. Furthermore, there is evidence for the microRNAs controlling gene expression in *Paulownia tomentosa* cambial tissues in response to seasonal changes [31].

Transcriptomic analyses have been carried out to profile gene expression regulations for biotic and abiotic stresses and growth responses. However, to the best of our knowledge, no study has described how the gene expression profile changes in woody tissues under seasonal variations. In this study, we sequenced and analyzed the transcriptomes of cambium tissues collected during the winter and spring seasons to assess the impact of two seasons on biomass. A transcriptome-wide analysis identified 61,639 annotated unigenes, and 2688 and 7411 transcripts were up- and downregulated, respectively, in the spring

season. Interestingly, among the selected wood-forming genes, hemicellulose-specific genes were upregulated in spring. Finally, 11,338 simple sequence repeats (SSRs) were identified from the transcriptome data. The identification of genes and pathways involved in cambial growth will be useful to further investigate the regulation of wood formation in Paulownia and other trees.

## 2. Materials and Methods

### 2.1. Tissue Sampling and RNA Isolation

Samples were selected from trees growing at the Fort Valley State University (FVSU) Paulownia Bioenergy Farm located at 32° 31'15.04" N and 83° 52'12.95" W. Paulownia trees bear flowers first, and after 3–4 weeks of flowering, leaves appear. Samples in replicates were collected from two seasonal points, each representing a different physiological state. The first sample (winter wood; hereafter referred to as WW) was collected before flowering on 1 March 2015 (min temp 33.1 °F and max temp 54 °F) and represented the senescent winter wood (Figure 1A). The second sample (spring wood; hereafter referred to as SW) was collected on 20 May 2015 (min temp 64 °F, max temp 91 °F) during spring and was representative of the actively growing spring wood (Figure 1B). Samples were harvested from twigs located at approximately 1.0–1.5 m from the ground with an average diameter of 2.5 cm. Since Paulownia has an opposite branching pattern, the WW and SW samples were taken from the mirrored axis of nodes. The samples were labeled, wrapped in aluminum foil, flash-frozen in liquid nitrogen, and subsequently stored in a –80 °C freezer until further use. Biological replicates were labeled as WW1, WW2, and WW3 for WW, and SW1, SW2, and SW3 for SW, respectively.

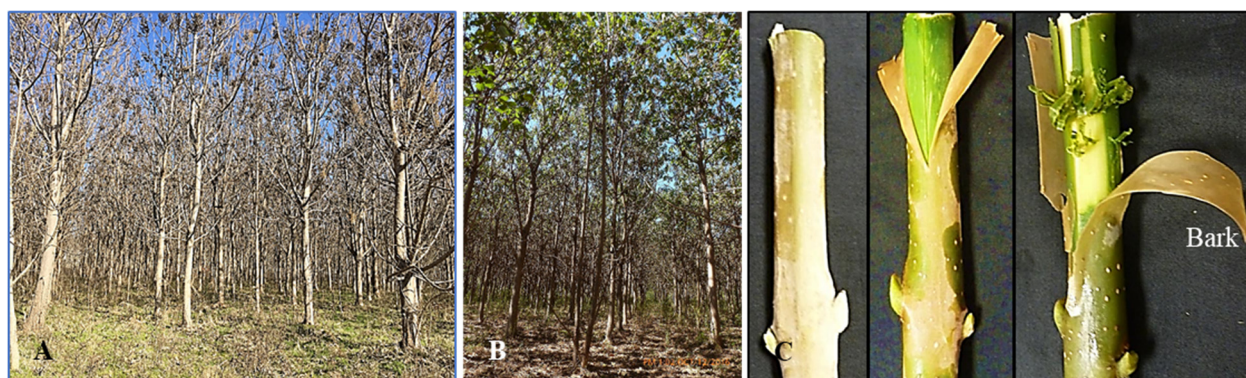


**Figure 1.** Six-year-old Paulownia trees growing at the ‘Paulownia Demonstration Plot’ at FVSU. Paulownia trees in dormant state during winter (A) and active state during spring (B). Cambial tissue sampling from a paulownia twig (C); normal branch (left), branch after bark removal (middle), and scraping wood forming cambial tissue for RNA extraction (right).

For high-quality, intact total RNA extraction, vascular cambium tissues were harvested from the frozen samples by first slicing a shallow, longitudinal cut into the outer bark with a sterile scalpel (Figure 1C). The bark was then removed using sterile forceps in a large, single piece. The frozen green vascular cambium was then gently scraped from the wood below into small strips using a sterile scalpel. A 100 mg vascular cambium tissue sample was powdered into microvials containing zirconia beads (BioSpec, Bartlesville, OK, USA) and 550 µL of TRIzol reagent (Invitrogen, Carlsbad, CA, USA) in a MagNA Lyser (Roche, Basel, Switzerland) as described earlier [32]. RNA was purified using Direct-Zol™ RNA mini-prep kit (Zymo Research, Irvine, CA, USA), and removal of genomic DNA contamination was carried out using DNase I treatment. RNA quality and quantity were analyzed using NanoDrop 1100 (NanoDrop, Wilmington, DE, USA) and Agilent 2100 Bioanalyzer (Agilent, Santa Clara, CA, USA).

## 2.2. cDNA Synthesis and RNA Sequencing

RNA samples of each biological replicate from both treatments (a total of 6 samples) were sequenced at BGI International (<http://bgi-international.com/>). Briefly, magnetic beads coated with Oligo (dT) were used to isolate mRNA from the total RNA, and size selected mRNA were adapter-ligated and sequenced on the Illumina Hiseq 2000 platform following the manufacturer's protocol.

## 2.3. Assembly and Annotation

Raw reads generated from pair-end sequencing were filtered for adapters and low-quality sequences by BGI proprietary software "filter\_fq". Clean reads were assembled into transcripts using Trinity (<http://trinityrnaseq.sourceforge.net/>) [33]. Three modules in Trinity (*Inchworm*, *Chrysalis*, and *Butterfly*) were applied sequentially to process raw RNA-seq reads to assemble them into contigs and full-length transcripts (unigenes). Butterfly also determined alternatively spliced isoforms of genes. Unigenes were aligned with five databases, namely, KEGG (Kyoto Encyclopedia of Genes and Genomes), COG (Clusters of Orthologous Groups), NT (NCBI nucleotide database), NR (NCBI non-redundant protein database), and Swiss-Prot (Protein sequence database). The KEGG database [34] was used to perform a systematic analysis of metabolic pathways and the function of gene products within a cell. The COG database (<http://www.ncbi.nlm.nih.gov/COG/>) was used to classify orthologous gene products into clusters. COG clusters predicted the possible function of the transcripts. Both NCBI's NR database and the Swiss-Prot (<http://www.uniprot.org/uniprot/>) annotated protein databases and added additional information about the possible function of the transcripts.

## 2.4. Gene Ontology and Coding Sequences

Gene ontology (GO) was employed to standardize functional gene classification, including molecular function, cellular components, and biological processes. The Blast2GO program (<http://www.blast2go.com/b2ghome>) was used to retrieve GO functional classification for all transcripts [35]. In order to determine the CDS for the transcripts, unigenes were first aligned to the protein databases, listed in order of priority of NR, Swiss-Prot, KEGG, and COG by using a local blastx (<ftp://ftp.ncbi.nlm.nih.gov/blast/executables/release/LATEST/>), with a significant cut-off value of  $e^{<0.00001}$ , of the unigene sequences. Unigenes with alignments to higher priority databases, for example, the NR database, were not aligned to lower priority databases. The highest-ranking proteins in the blastx results were used to decide the coding region sequences of unigenes. Results of the blastx alignment used a standard codon table to translate the nucleotide query sequence into a translated amino acid sequence. Unigenes that could not be aligned to any database were further scanned by ESTScan [36], producing nucleotide sequence (5'→3') direction and amino sequence of the predicted coding region.

## 2.5. Gene Expression Analysis

In order to determine the expression pattern of the unigenes, clean reads were first mapped to unigenes using the program Bowtie2 (v. 2.2.5) [37]. SAM files generated through Bowtie were used with the RSEM (RNA-Seq by Expectation-Maximization) software package (<http://deweylab.github.io/RSEM/>; v1.2.12) in R (v1.03; <http://www.r-project.org/>) to measure the expression level of unigenes. RSEM software was used to estimate gene expression levels from RNA-seq data [38] in FPKM (fragments per kilobase of transcript per million mapped reads) format, which was subsequently used to perform differential gene expression analysis in this study. To detect differentially expressed genes (DEGs), the program NOIseq was utilized [39]. In this study, WW and SW unigenes with a fold change of  $\geq 2$  and a probability  $\geq 0.8$  were considered to be significantly differentially expressed. Principal component analysis (PCA) was performed using the R statistical package.

## 2.6. Simple Sequence Repeats Analyses

Simple sequence repeat (SSR) identification was accomplished with MicroSATellite (MISA) software (<http://pgrc.ipk-gatersleben.de/misa/misa.html>), using unigenes as input sequences. The identified SSRs with nucleotide size > 150 bps on both ends of the unigenes were used for oligonucleotide design using Primer3 (v2.3.4; <http://www.onlinedown.net/soft/51549.htm>).

## 2.7. Validation of Wood-Forming Candidate Genes with RT-qPCR

Based on existing research information, fifteen wood-forming candidate genes corresponding to the biosynthesis of cellulose, hemicellulose, or lignin [18,40–43], were selected for validation of expression level. Using the local blast utility (<ftp://ftp.ncbi.nlm.nih.gov/blast/executables/release/LATEST/>), a database of all Paulownia unigenes was created. The mRNA sequences acquired for each of the selected genes were then aligned to the database of all unigenes using the local blastx utility. The unigenes showing maximum homology for each of the genes were selected for a two-step RT-qPCR primer design. The software Primer Express v3.01 (Applied Biosystems, Foster City, CA) was used to design primers for the unigenes corresponding to the selected wood forming genes. cDNA was synthesized from Paulownia vascular cambium total RNA using SuperScript™ II Reverse Transcriptase (Invitrogen, Waltham, Massachusetts, USA) with the suggested protocol. FastStart SYBR Green Master Mix (Roche, Grenzachstrasse, Basel, Switzerland) reagent was used in combination with primers and cDNA. RT-qPCR of three biological replications with no-template control (NTC) involved StepOnePlus Real-Time PCR System (Applied Biosystems, Foster City, CA, USA) and FastStart SYBR Green (Roche). The expression of selected genes was normalized with reference gene 18S rRNA. Finally, the relative gene expression was measured using the  $2^{-\Delta\Delta C_t}$  method [44].

All raw files of sequencing data have been submitted to the NCBI Sequenced Read Archive (SRA) database with accession numbers SRX9298494—SRX9298499.

## 3. Results and Discussion

### 3.1. RNA-Seq and Transcriptome Assembly of Paulownia Cambial Tissue

To obtain the candidate genes associated with cambium development of the empress tree (common name for all Paulownia species) during seasonal growth, transcriptome sequencing analysis for tissues representing winter and spring seasons (Figure 1A,B) was carried out by collecting cambial tissues from tree twigs (Figure 1C). A total of 305,882,370 (~29 Gb) raw reads were generated. Removal of adapter sequences, low-quality reads, and ambiguous sequences resulted in 297,049,842 clean reads (Q20 > 97.73%) with an average length of 100 nucleotides. WW generated more raw reads when compared to spring wood samples (Table 1). The de novo assembling of clean reads produced 129,428 and 104,388 contigs for WW and SW cambial tissues, respectively. Clustering and assembly of these contigs resulted in 64,142 and 45,671 unigenes for WW and SW with an average length of 960 and 842 nucleotides, respectively. Among the unigenes, all unigenes were sub-classified according to nucleotide length (Figure S1). A total of 40,814 unigenes were greater than 1 Kbs, and 58,654 unigenes were greater than 500 nucleotides in length. The mean length of the contigs (~340 bp) was shorter than that of the unigenes (>1000 bp) in most previously reported studies. The paired-end reads resulted in longer unigenes (average of ~900 bp) than those reported in previous transcriptome studies on trees [45,46]. The mean length of unigenes (900 nucleotides) was less than those reported in previous studies on tetraploid *Paulownia australis* and drought exposed *P. tomentosa* [23,47]. Most of our assembled unigenes showed homology to nucleotide sequences deposited in six public nucleotide databases. The unmatched unigenes are most likely to represent Paulownia-specific genes especially related to the winter and spring seasons.

**Table 1.** Summary of the sequence assembly after Illumina sequencing and statistics of contigs and unigenes ( $n = 3$ ). The values are given as Mean  $\pm$  SD from three replications.

	Winter Wood	Spring Wood
Total raw reads	51,005,253 $\pm$ 2,639,904	52,359,187 $\pm$ 737,515
Total clean reads	49,766,422 $\pm$ 2,349,991	50,689,696 $\pm$ 1,090,856
Percentage of reads	97.60 $\pm$ 0.52	96.64 $\pm$ 0.63
Q20 Percentage	97.96 $\pm$ 0.36	97.51 $\pm$ 0.35
Contigs		
Total Number	129,428 $\pm$ 610	104,388 $\pm$ 1779
Total Length (nt)	43,730,308 $\pm$ 513,387	35,501,692 $\pm$ 721,304
Mean Length (nt)	338 $\pm$ 3	340 $\pm$ 1
N50	605 $\pm$ 7	642 $\pm$ 4
Unigenes		
Total Number	64,142 $\pm$ 1229	45,671 $\pm$ 1225
Total Length (nt)	61,610,800 $\pm$ 2,101,797	38,465,680 $\pm$ 1,457,846
Mean Length (nt)	960 $\pm$ 14	842 $\pm$ 9
N50	1551 $\pm$ 25	1354 $\pm$ 22

### 3.2. Functional Annotation of Paulownia Cambial Transcriptome

A total of 61,639 transcripts were annotated by performing a BLAST search of the sequences across six databases as described above. The BLAST search using 61,639 transcripts showed 72.47% similarity to non-redundant (Nr) protein database (Tables S1 and S2).

Of the annotated sequences in the Nr database, 39.3% of the mapped unigenes had very significant homology to known sequences ( $e$ -value 10–100), 35.1% showed significant homology (10–100;  $e$ -value 10–30), and 25.6% showed weak homology ( $e$ -value 10–30 to 10–5) (Figure 2A). We also performed the sequence conservation analysis of Paulownia transcripts with proteomes of all sequenced plant species. As depicted in Figure 2B, the E-value distribution analysis of transcripts showed that 47.0% of unigenes had a similarity of more than 80% with plant species. We used a BLAST search to study the relationship of Paulownia with other plant species to identify proteins and pathways that would be unique to Paulownia. The sequence conservation analysis of transcripts showed homology to nucleotide sequences from *Erythranthe guttata* (64.8%), followed by *Vitis vinifera* (6.3%), *Solanum tuberosum* (5.0%), *Solanum lycopersicum* (3.0%), *Theobroma cacao* (2.7%), and others (Figure 2C). *Erythranthe guttata*, a yellow bee-pollinated annual or perennial plant, is a model organism for biological studies. Paulownia transcripts shared strong homology with *Erythranthe* species, and this could be due to close phylogenetic relationships between these two species [48]. However, transcripts from a drought-related transcriptomic study of Paulownia [28,47] showed homology to *Vitis vinifera* (45–48%), which could be due to the selection of seasonal abiotic tissue for cambial transcriptome study.

Further analysis of 43,780 transcripts using the COG database classified these transcripts into 25 different protein families with potential functions in transcription, replication and recombination, posttranslational modification, signal transduction, and others.

Interestingly, only a few transcripts exhibited their potential role in the extracellular structure and nuclear structure (17 and 4 transcripts, respectively). Importantly, many unigenes have been assigned to a wide range of COG classifications (Figure 3), indicating that a wide diversity of transcripts were involved in wood formation as in Chinese fir [31].

The Gene Ontology (GO) classification classified 42,588 out of 62,639 transcripts into ontologies related to molecular functions, cellular components, and biological processes (Figure 4). We identified a significantly higher number of transcripts involved in metabolic processes (19,418) and related to cellular processes (18,047) when compared to others, such as rhythmic processes. The most represented category for cellular components was cells (GO: 0005623; 18,186 genes), followed by organelles (GO:0043226; 14,053 genes). Genes and pathways putatively responsible for dormant winter and active spring growth in Paulownia were identified in this study. In *Populus*, *PtrHB7*, a class III HD-Zip gene, is known to play a critical role in the regulation of vascular cambium differentiation [49] and homeobox gene

*ARBORKNOX1* regulates the shoot apical meristem and the vascular cambium [50]. In our study, Unigene2201, Unigene3374, and Unigene4121 which were downregulated in their expressions, belong to GO:0005488 (molecular function: binding) and are homologs of the *KNOX* gene. *KNOX* family gene *KNAT7* negatively regulates secondary wall formation in *Arabidopsis* and *Populus* [51]. Since *KNAT7* is a negative regulator of secondary wall biosynthesis, these *Paulownia* homologs might positively regulate cambium growth during the active spring season.

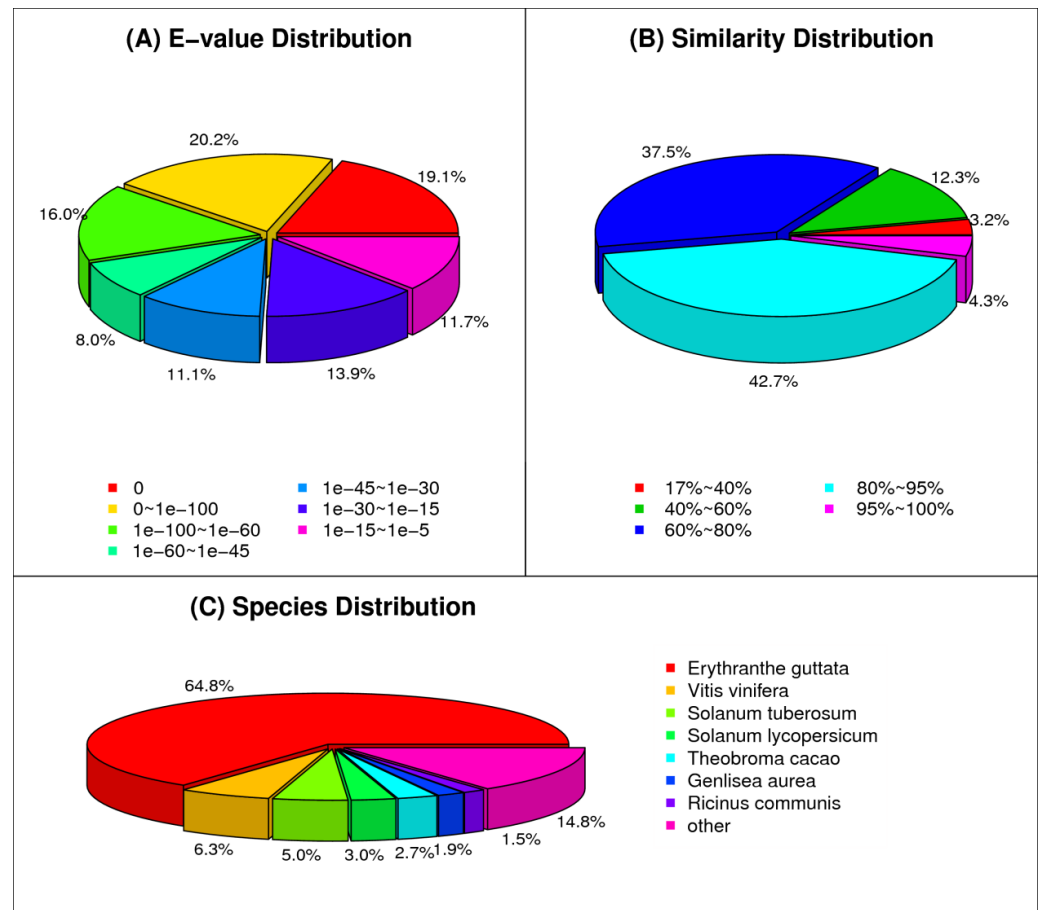


**Figure 2.** Statistics of homology search of unigenes against Non-redundant (NR) protein database. Distribution of top BLASTX hits with cut-off  $e$ -value of  $<1.0 \times 10^{-5}$  (A), similarity (B), and species distributions (C) of all unigenes.

KEGG annotation yielded a total of 35,471 (57.5%) transcripts that were mapped to 128 KEGG pathways. The top three KEGG enriched pathways were metabolic pathways (7943 transcripts; 22.39%; ko01100), biosynthesis of secondary metabolites (3768 transcripts; 10.62%; ko01110), and plant-pathogen interaction (1852 transcripts; 5.22%; ko04626 (Tables S3 and S4). With the help of the KEGG database, we could further analyze the metabolic pathways and functions of gene products, which can help in studying the complex biological behaviors of genes. The majority of representative unigenes were annotated to metabolic pathways, biosynthesis of secondary metabolites, plant-pathogen interaction, plant hormone signaling, spliceosome, and phenylpropanoid biosynthesis using the KEGG database, which led us to conclude that most of the genes identified in this study are involved in cambial differentiation and wood formation.

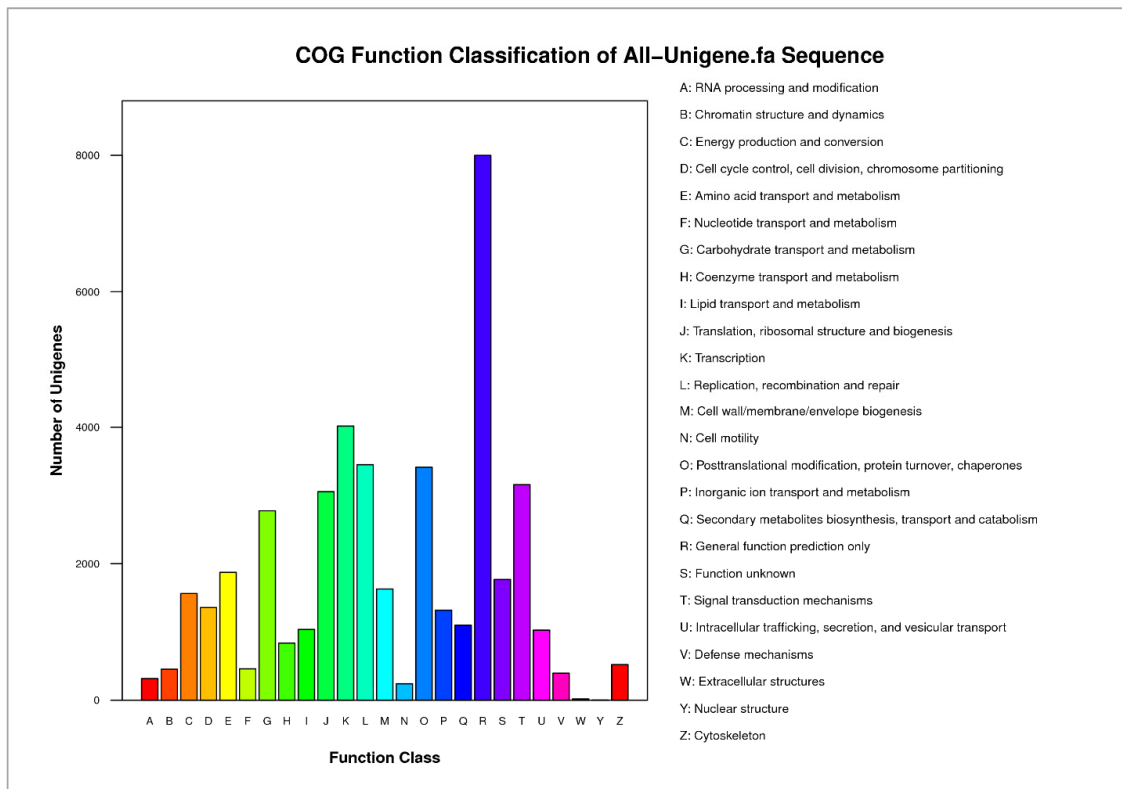


**Figure 3.** Histogram representation of clusters of orthologous groups (COG). The horizontal coordinates are function classes of COG, and the vertical coordinates are numbers of unigenes in one class. The notation on the right is the full name of the functions in the *x*-axis. Histogram representation of classification of the clusters of orthologous groups (COG) for the total aligned 43,780 unigenes (53.43%) into 25 functional groups.

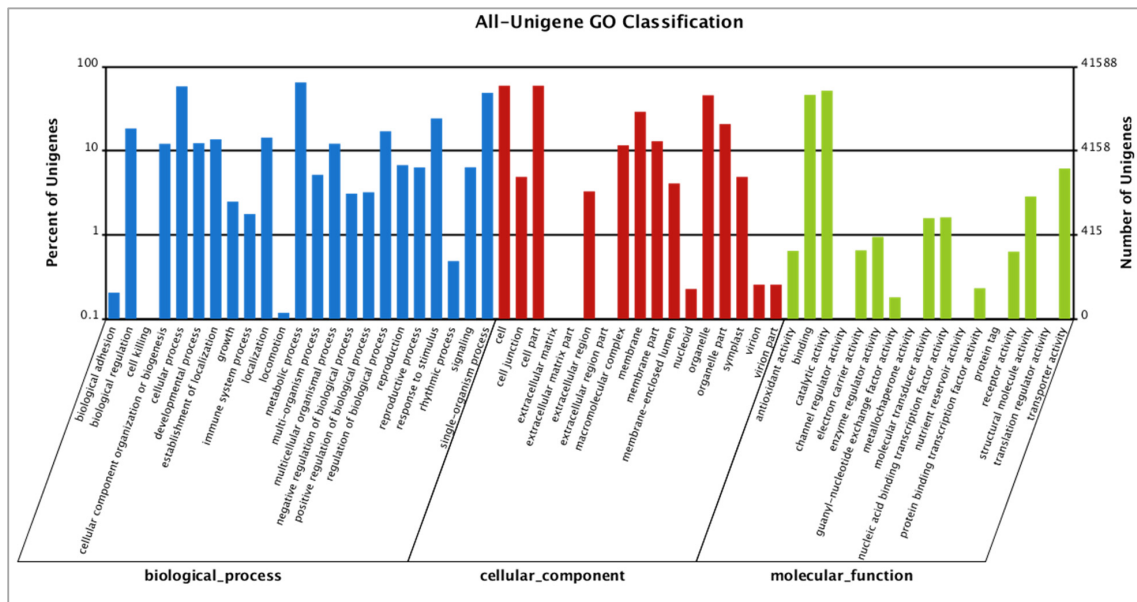


**Figure 4.** GO classification analysis of unigenes. GO functions are showed on the *x*-axis. The right *y*-axis shows the number of genes that have the GO function, and the left *y*-axis shows the percentage. Unigenes in the winter and spring season are classified into biological processes, cellular components, and molecular functions. In total, 41,588 (50.76% of all unigenes) were assigned to 48 GO categories.

### 3.3. Transcriptional Profiling of Cambial Tissues in Winter and Spring

A total of 10,099 (12.33%) transcripts were found to be significantly differentially expressed between two tissue samples. Of these differentially expressed genes (DEGs), 2688 (26.61%) transcripts were found to be upregulated (>1.6 fold) in the spring season, whereas 7411 (73.39%) were downregulated (<−1.6 fold) when compared to the winter season (Figure S2). Hierarchical clustering of the DEGs identified in winter and spring conditions led to the detailed overall structure of clustering. This indirectly indicated that more genes were upregulated, active, and required during the senescent winter season to keep tissues dormant. Out of 2688 genes, the top 20 genes with  $\log_2$ Fold change >8.00 are summarized in Table 2. This included APC/C cyclosome complex, phosphoenolpyruvate carboxykinase, different classes of heat shock proteins, actin depolymerization factor, anaphase-promoting complex subunit (>12-fold expression), etc. Similarly, many key genes, including synthases such as galactinol synthase (<−12-fold expression), rosmarinic acid synthase, and valencene synthase, kinases such as receptor-like protein kinase, serine/threonine-protein kinase, CBL-interacting protein kinase, and hormone-regulated genes such as auxin efflux carrier family protein and ethylene-responsive transcription factor were downregulated (Table 3). The cell cycle is one of the most important biological processes in the cambial zone and plays a central role in regulating the growth and development of organisms, including plants. The anaphase-promoting complex/cyclosome (APC/C; homolog in our study Unigene8688), a well-known ubiquitin ligase, acts to accomplish basic cell-cycle control. The APC/C must be turned off at the end of the G1 phase to allow the S phase cyclins to accumulate and cells to begin DNA replication [52]. This is very key during the spring season for cell multiplication and growth. The *Cyclin U2* (Unigene22553), one of the major cyclins involved in cell cycle control, like cyclins A and B on maximum gene expression in the poplar cambium zone [53], was upregulated in Paulownia. The high abundance of cyclin transcripts in active cambium during the spring season also reflected a positive correlation between cambium cell division and key cell cycle gene expression.

**Table 2.** List of top 20 upregulated known genes.

Unigene/Contig	Length	WW Expression	SW Expression	$\log_2$ Fold Change (SW/WW)	Probability	Gene
Unigene8688	995	0.01	42.67	12.06	0.9997	Anaphase-promoting complex, cyclosome, subunit 4
Unigene11861	477	0.01	27.14	11.41	0.9994	Heat shock protein
Unigene6740	2339	0.01	17.72	10.79	0.9989	Phosphoenolpyruvate carboxykinase
Unigene1612	1191	0.01	11.95	10.22	0.9978	Cysteine-type peptidase activity
Unigene3797	247	0.01	8.11	9.66	0.9953	Calcium-binding domain
Unigene10820	977	0.03	24.79	9.54	0.9992	Class IV heat shock protein
Unigene17843	560	0.01	6.50	9.34	0.9926	Pericarp peroxidase
Unigene1476	971	0.01	6.17	9.27	0.9918	Sulfated surface glycoprotein
Unigene11860	940	0.10	58.64	9.24	0.9996	Class I heat shock protein
Unigene34010	359	0.01	5.87	9.20	0.9910	Photosystem II oxygen-evolving complex protein 2 precursor
Unigene15576	532	0.01	5.42	9.08	0.9893	Gibberellin-regulated protein
Unigene35083	779	0.82	359.96	8.78	0.9995	Heat shock protein
Unigene1551	276	0.01	4.14	8.69	0.9814	Large subunit ribosomal protein
Unigene8720	500	0.01	4.08	8.67	0.9808	Actin-depolymerizing factor
Unigene19860	1028	0.01	4.01	8.65	0.9801	Leucine-rich repeat extensin
Unigene4065	510	0.01	4.00	8.64	0.9801	Actin depolymerization factor
Unigene4063	527	0.06	23.35	8.60	0.9986	Aquaporin PIP2
Unigene3966	521	0.01	3.62	8.50	0.9754	Tubulin/FtsZ family
Unigene8766	606	0.01	3.59	8.49	0.9750	Class II heat shock protein
Unigene11017	503	0.01	3.54	8.47	0.9742	Cyclophilin peptidyl-prolyl cis-trans isomerase

**Table 3.** List of top 20 downregulated genes.

Unigene/Contig	Length	WW Expression	SW Expression	log <sub>2</sub> Fold Change (SW/WW)	Probability	Gene
Unigene22837	205	73.99	0.01	−12.85	0.9998	Galactinol synthase
Unigene6926	252	21.15	0.01	−11.05	0.9991	MATE efflux family protein
CL7319.Contig2	890	16.20	0.01	−10.66	0.9987	Coproporphyrinogen-III oxidase
Unigene13375	584	14.56	0.01	−10.51	0.9985	Rosmarinate synthase
Unigene10966	1645	11.55	0.01	−10.17	0.9977	Receptor-like protein kinase
Unigene10726	1857	8.84	0.01	−9.79	0.9961	Valencene synthase
CL698.Contig3	3901	6.65	0.01	−9.38	0.9929	Pectin methyltransferase
CL8528.Contig1	1476	6.63	0.01	−9.37	0.9929	Root phototropism protein
CL7708.Contig2	888	6.54	0.01	−9.35	0.9927	Splicing factor U2af large subunit
CL889.Contig1	1018	6.46	0.01	−9.33	0.9925	Tropinone reductase homolog
CL7009.Contig1	1844	6.39	0.01	−9.32	0.9924	Auxin efflux carrier family protein
Unigene13264	1617	6.04	0.01	−9.24	0.9915	Ethylene-responsive transcription factor
Unigene15599	228	5.86	0.01	−9.20	0.9909	Nitrate transporter
CL8637.Contig1	863	4.75	0.01	−8.89	0.9859	DNA repair protein RadA
CL799.Contig5	3446	4.72	0.01	−8.88	0.9857	Serine/threonine-protein kinase
Unigene1474	1021	4.55	0.01	−8.83	0.9845	Xanthoxin dehydrogenase
Unigene25603	518	4.52	0.01	−8.82	0.9844	SPX domain-containing membrane protein
Unigene6422	1304	45.72	0.10	−8.79	0.9993	Ethylene-responsive transcription factor
CL822.Contig5	1916	4.24	0.01	−8.73	0.9823	Putative dual-specificity protein phosphatase
Unigene13350	451	4.13	0.01	−8.69	0.9813	CBL-interacting protein kinase

As shown in Figure 5, GO analysis indicated that most of the differentially expressed transcripts for biological processes were involved in the metabolic process (1016), cellular process (890), and response to stimulus (350). Similarly, GO cellular component analysis revealed that a large number of transcripts encoded functions related to cell (824), cell part (789), membrane (436), and organelle (399) synthesis. Meanwhile, GO molecular function analysis showed that the DEGs predominantly contributed to catalytic activity (836), followed by transporter activity and structural molecule activity. KEGG enrichment analysis of DEG showed that these genes were involved in various pathways in the Paulownia plant during seasonal changes (Table 4). Most of the DEGs were enriched in metabolic pathways (ko01100; 1387), biosynthesis of secondary metabolites (ko01110; 827), and plant hormone signal transduction (ko04075; 320). It was also found that starch and sucrose metabolism (ko00500; 172; Figure S3) and phenylpropanoid biosynthesis (ko00940; 106; Figure S4), which correspond to the production of several key wood-forming genes, were within the top 25 most DEG enriched KEGG pathways (Table 4). Nineteen (Unigene11539, Unigene12164, Unigene12788, Unigene16018, Unigene17615, Unigene18048, Unigene18594, Unigene18926, Unigene22808, Unigene24462, Unigene24837, Unigene3634, Unigene4753, Unigene6221, Unigene891, and Unigene9670 (K00430), Unigene16856 (K11188), Unigene22599 and Unigene25305 (K03782)) out of 497 unigenes (total unigenes) involved in lignin synthesis in the phenylpropanoid biosynthesis pathway (Ko00940) were identified and differentially regulated (Figure S4). Lignin plays a vital role in keeping the structural integrity of the cell wall and protecting plants from pathogens [54], as well as a main component of wood. Of these 19, different types of peroxidases (Unigene11539, Unigene18926, Unigene4753 and Unigene6221) were upregulated during winter. Recently, a notable remodeling of the transcriptome was reported in Norway Spruce, where monolignol biosynthesis genes showed high expression during the period of secondary cell wall formation as well as the second peak in midwinter. Interestingly, this midwinter peak expression did not trigger lignin deposition [55]. These genes could be preparing for the biosynthesis and distribution of guaiacyl (G), p-hydroxyl phenol (H), and syringyl (S) lignin in developing biomass as soon as the onset of spring.

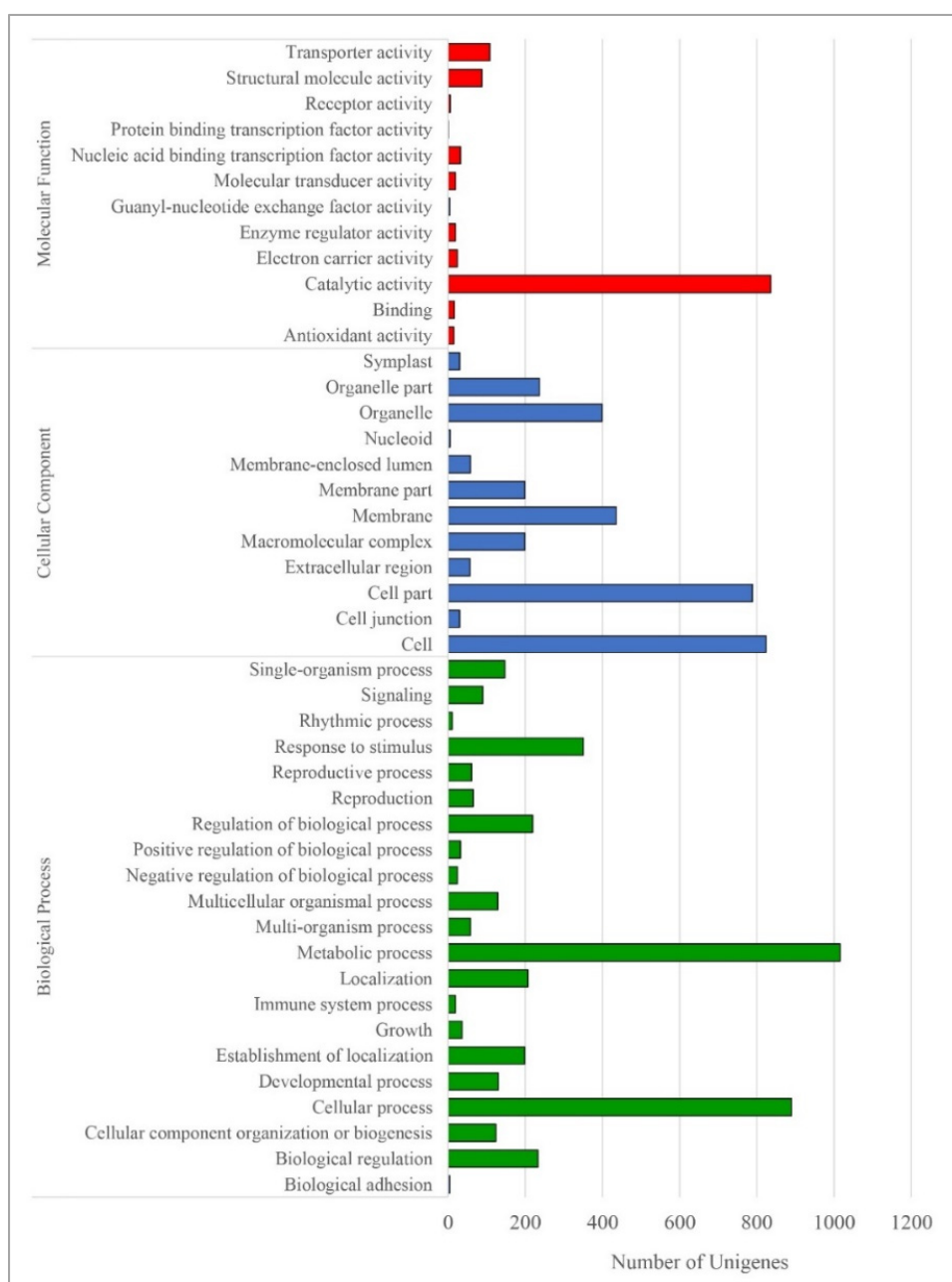


**Figure 5.** GO function analysis of the differentially expressed genes. GO function analysis results for the differentially expressed genes in cambial tissues due to winter and spring seasons into biological processes, cellular components, and molecular functions.

**Table 4.** Top 25 DEG enriched KEGG pathways.

Pathway	Number of DEGs Genes	<i>p</i> -Value	Pathway ID
Metabolic pathways	1387	1.32E <sup>-12</sup>	ko01100
Biosynthesis of secondary metabolites	827	7.55E <sup>-10</sup>	ko01110
Plant hormone signal transduction	320	1.58E <sup>-05</sup>	ko04075
Plant-pathogen interaction	266	0.2430222	ko04626
Ribosome	204	0.200625	ko03010
Spliceosome	178	0.9468082	ko03040
Starch and sucrose metabolism	172	1.22E <sup>-06</sup>	ko00500
Protein processing in E.R.	162	0.3255727	ko04141

Table 4. Cont.

Pathway	Number of DEGs Genes	<i>p</i> -Value	Pathway ID
Carbon metabolism	161	0.04321163	ko01200
RNA transport	151	0.986695	ko03013
Glycerophospholipid metabolism	138	0.1244536	ko00564
Endocytosis	134	0.6458048	ko04144
Biosynthesis of amino acids	123	0.7258124	ko01230
Glycolysis/Gluconeogenesis	115	5.48E <sup>-05</sup>	ko00010
Phenylpropanoid biosynthesis	106	1.50E <sup>-06</sup>	ko00940
Circadian rhythm—plant	105	5.10E <sup>-09</sup>	ko04712
Ether lipid metabolism	104	0.02664109	ko00565
Ubiquitin mediated proteolysis	99	0.7266876	ko04120
Pentose and glucuronate interconversions	93	1.57E <sup>-05</sup>	ko00040
Purine metabolism	92	0.9911015	ko00230
Amino sugar and nucleotide sugar metabolism	86	0.006516035	ko00520
Pyrimidine metabolism	78	0.992583	ko00240
mRNA surveillance pathway	77	0.9938776	ko03015
Flavonoid biosynthesis	70	8.18E <sup>-07</sup>	ko00941
RNA degradation	68	0.940714	ko03018

### 3.4. Expression of Lignocellulosic Pathway Genes and Their Validation

Wood, the secondary xylem, is produced from the activity of vascular cambium that is composed of two meristematic initials, fusiform and ray initials [56], with the sequential developmental process including differentiation of vascular cambium cells into secondary xylem mother cells, cell expansion, and massive deposition of secondary walls (where a number of genes involved in vascular tissue differentiation and secondary wall biosynthesis are) [57]. When the wood compression starts, the expression of a number of genes involved in the synthesis of lignocellulosic components (cellulose, hemicellulose, and lignin) and lignans was upregulated in maritime pine [58]. In addition, the onset of wood formation undergoes three periods: winter shrinkage, spring rehydration (32–47 days), and summer transpiration in the stem [59].

In order to explore the roles of cell wall- and hormone-related genes for the seasonal cues, fifteen candidate genes were identified from previous studies (Table 5). They are involved in cellulose (*CesA1*, *CesA3*, *CesA6* [60]), hemicellulose (*CSLC4* [61], *FUT1* [62,63], *AXY4* [64], *GATL1* [65], *IRX10* [66], *ESKIMO1* [67]), lignin (*4CL* [68], *CCR1* [69], *CAD1* [70]), auxin (*TAA1* [71], *YUC1* [72,73]), and cytokinin (*IPT1* [29] synthesis/pathways). RT-qPCR was employed to study the expression of these wood formation genes in Paulownia during the winter and spring seasons (Figure 6). Cellulose is synthesized in plant cell walls by large membrane-bound protein complexes proposed to contain several copies of the catalytic subunit of the cellulose synthase, *CesA*. Here, we found *CesA1* and *CesA6* were upregulated during spring while *CesA3* was moderately downregulated during the winter season. In hybrid aspen, expression analyses of the *CesA* family showed a specific location in normal wood undergoing xylogenesis, while *PttCesA2* seems to be activated on the opposite side of a tension wood [60]. However, in Arabidopsis, the expression levels of the three primary cell wall genes (*AtCesA2*, *AtCesA5*, *AtCesA6*) was increased, but not *AtCesA3*, *AtCesA9* or secondary cell wall *AtCesA7* [74]. Our results, along with these studies, indicated that the expression of major primary wall *CesA* genes accelerate the primary wall *CesA* complex.

Several proteins encoded by the cellulose synthase-like (*CSL*) gene family, including *CSLA* proteins, which synthesize  $\beta$ -(1→4)-linked mannans, and *CSLC* proteins, which are thought to synthesize the  $\beta$ -(1→4)-linked glucan backbone of xyloglucan are known to be involved in the synthesis of cell-wall polysaccharides [61]. Higher expression of *CSLC4* in Paulownia during the spring season indicated that it might involve cellulose synthesis. The fucosyltransferase (*FUT1*) is an enzyme that transfers an L-fucose sugar from a GDP-fucose (guanosine diphosphate-fucose) donor substrate to an acceptor substrate. The Arabidopsis *mur1* (*AtFUT1*) mutant study [63] exhibited a dwarf growth habit

and decreased wall strength indicating the indispensable role of FUT1 function in wood formation. Another key gene family of O-acetyl substituents seems to be very important for various plant tissues and during plant development [75], suggesting an important functional role in the plant. Mutants lacking *AXY4* transcript resulted in a complete lack of O-acetyl substituents on xyloglucan in several tissues, except seeds [64]. Biosynthesis of xylan in woody plants is a major pathway for plant biomass. *Populus* genes *PdGATL1.1* and *PdGATL1.2*, the closest orthologs to the Arabidopsis *PARVUS/GATL1* gene, have been shown to be important for xylan synthesis but may also have a role(s) in the synthesis of other wall polymers [65]. The expression of *GATL1* homolog was six-fold increased (Figure 6) in the spring season tissue of Paulownia, implying more xylan biosynthesis. Collapsed xylem phenotypes of Arabidopsis [76] and *Physcomitrella patens* [66] mutants (*irx10*) identified mutants deficient in cellulose deposition in the secondary cell wall due to lack of synthesis of the glucuronoxylan. Acetyl transferases are involved in cellulose biosynthesis in plants. In Arabidopsis, the *ESKIMO1 (ESK1)* gene participated in several functions, and *esk1 mutants* indicated that *ESK1* is necessary for the synthesis of functional xylem vessels in forming secondary cell wall components [67]. Our RNA seq data indicated that all the genes associated with cellulose and hemicellulose synthesis were expressed during the spring season to complete wood formation.

**Table 5.** Wood-Forming Genes Selected for RT-qPCR Expression Validation.

Gene Name	Unigene/Contig	Macromolecule	Enzyme/Protein Name	Activity	Function
<i>CESA3</i>	Unigene9908	Cellulose	Cellulose synthase A catalytic subunit 3 [UDP-forming]	Cellulose synthase	Catalytic subunit of cellulose synthase terminal complexes required for cell wall formation.
<i>CESA1</i>	Unigene21132	"	"	"	"
<i>CESA6</i>	Unigene13924	"	"	"	"
<i>CSLC4</i>	CL7362.Contig2	Hemicellulose	Xyloglucan glycosyltransferase 4	Glucan synthesis	Involved in the synthesis of the xyloglucan backbone.
<i>FUT1</i>	Unigene2841	Hemicellulose	Galactoside 2- $\alpha$ -L-fucosyltransferase	Fucosyl transferase	Addition of the terminal fucosyl residue on xyloglucan side chains. Involved in xyloglucan-specific O-acetylation in roots and rosette leaves.
<i>AXY4</i>	Unigene14391	Hemicellulose	Protein ALTERED XYLOGLUCAN 4	Acetyl transferase	
<i>GATL1</i>	Unigene14440	Hemicellulose	Galacturonosyltransferase-like 1	Xylan synthase	Family 8 glycosyl transferase that contributes to xylan biosynthesis.
<i>IRX10</i>	Unigene2644	Hemicellulose	Beta-1,4-xylosyltransferase	Xylan synthase	Synthesis of the hemicellulose glucuronoxylan, a major component of secondary cell walls. Xylan acetyltransferase required for 2-O- and 3-O-monoacetylation of xylosyl residues in xylan.
<i>ESKIMO1</i>	CL7514.Contig1	Hemicellulose	Protein ESKIMO 1	Acetyl transferase	Produces CoA thioesters of a variety of hydroxy- and methoxy-substituted cinnamic acids.
<i>4CL</i>	CL764.Contig3	Lignin	4-coumarate-CoA ligase 1	Monolignol synthesis	Involved in monolignol biosynthesis, the conversion of cinnamoyl-CoAs into cinnamaldehydes.
<i>CCR1</i>	CL6693.Contig1	Lignin	Cinnamoyl-CoA reductase 1	Monolignol synthesis	Involved in lignin biosynthesis. Catalyzes the final step specific for the production of lignin monomers.
<i>CAD1</i>	Unigene17183	Lignin	Cinnamyl alcohol dehydrogenase 1	Monolignol synthesis	Performs first two reactions in auxin pathway.
<i>TAA1</i>	CL8952.Contig1	Auxin	L-tryptophan-pyruvate aminotransferase 1	Auxin synthesis	Catalyzes the N-oxidation of tryptamine to form N-hydroxyl tryptamine.
<i>YUC1</i>	CL1596.Contig1	Auxin	Indole-3-pyruvate monoxygenase YUCCA1	Auxin synthesis	Catalyzes the transfer of an isopentenyl group from dimethylallyl diphosphate (DMAPP) to ATP, ADP, and AMP.
<i>IPT1</i>	Unigene8131	Cytokinin	Adenylate isopentenyltransferase 1, chloroplastic	Cytokinin synthesis	

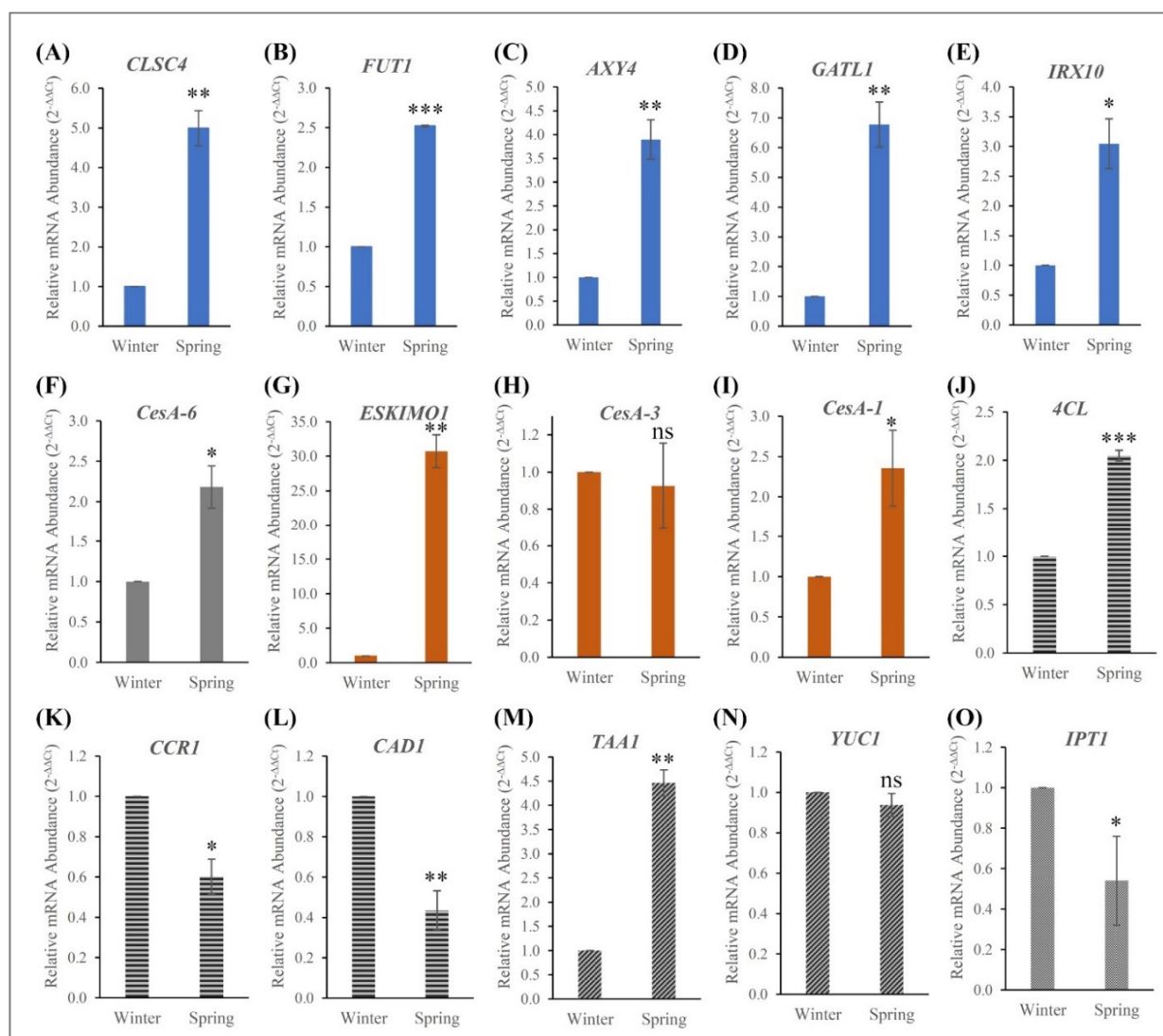


**Figure 6.** Relative mRNA expression of key genes involved in winter and spring seasons (A–O). Expression of genes involved in cell wall synthesis (*CLSC4*, *FUT1*, *AXY4*, *GATL1*, *IRX10*, *CesA-6*, *ESKIMO1*, *CesA-3*, *CesA-1*, *4CL*, *CCR1*, and *CAD1*) (A–L) and hormone synthesis (*TAA1*, *YUC1*, *IPT1*) (M–O). Expression quantity of the calibrator sample (winter tissue) was set to 1. Data are the mean  $\pm$  SD. Student's *t*-test was used to compare significant changes in spring tissues compared to winter tissues. \*,  $p < 0.1$ ; \*\*,  $p < 0.01$ ; \*\*\*,  $p < 0.001$ ; ns, no significance.

### 3.5. Analysis of Hormone-Specific Genes and Their Validation

Plant growth regulator auxins play a key role in regulating wood formation through their action on cambial activity and xylem development [77]. Auxin has been shown to be required for maintaining the cambium in a meristematic state as depleting the auxin in cambium leads to differentiation of cambial cells into axial parenchyma cells [78]. Cytokinins, on the other hand, have a well-established function in cell division during growth and development, and they are called central regulators of cambial activity [79]. The interaction between auxin and cytokinin seems to be essential for the induction of phenylalanine ammonia-lyase activity in support of lignification [80]. *TAA1*, which performs the first two reactions in the auxin pathway, is a Trp aminotransferase that converts Trp to IPA in the IPA auxin biosynthesis branch in Arabidopsis [73]. Higher-order mutants in *TAA1* showed auxin-related multiple phenotypes. Later, it was identified that the *TAA1* gene was essential for hormone crosstalk with ethylene for plant development [71]. Later, new putative functions of IAA production via IPyA and transport were identified [81].

Another group of auxin biosynthesis gene family, *YUCCA* flavin monooxygenases, control the formation of floral organs and vascular tissues in *Arabidopsis* [72]. When the *TAA* family of aminotransferases converts tryptophan to indole-3-pyruvate (IPA), *YUCCA* (*YUC*) family participates in converting IPA to IAA [73]. In addition, the authors found that *YUC* and *TAA* work genetically in the same pathway and that *YUC* is downstream of *TAA*. From our transcriptome and gene expression studies, we observed *TAA1* was strongly expressed, but *YUC1* expression was negligible during the spring season. Our study identified several transcripts involved in auxin biosynthesis through the tryptophan pathway for cell enlargement and plant growth (Figure S5).

In *Arabidopsis*, cambial activity responded to small changes in cytokinin levels indicating that cytokinins are central regulators of cambium activity [79]. Isopentenyltransferase, the rate-limiting step of cytokinin biosynthesis, is an important enzyme playing key roles in meristem maintenance and organ development. *Arabidopsis* quadruple mutants lacking *AtIPT1*, *AtIPT3*, *AtIPT5*, and *AtIPT7* were unable to form cambium and showed reduced thickening of the root and stem, though single mutant *atipt3* showed moderately decreased levels of cytokinins without any other recognizable morphological changes. Similarly, increased cytokinin biosynthesis stimulates the cambial cell division rate and increases the production of trunk biomass in transgenic *Populus* trees [29]. Surprisingly, *IPT1* expression was high in winter and moderately reduced in spring. There could be many other members in the *IPT* family that complements the function of cambial development. Auxin and cytokinin display distinct distribution profiles across the cambium, and elevated cytokinin content leads to an increased cambial auxin concentration [29]. Together, it is very interesting to see the interaction of lignocellulosic pathways genes along with major hormone-regulated genes and their cross-talks to maintain the balance of cambial activities for quality wood formation with alternative seasonal changes (Figure S6).

### 3.6. Analysis of Simple Sequence Repeats (SSRs)

SSR markers are very useful for multiple applications in plant genetics because of their co-dominance, high level of polymorphism, multi-allelic variance, and abundance, and cross-species transferability [82,83]. In the present study, SSR was identified utilizing the transcriptome of *Paulownia* cambial tissues because EST-SSR markers have a relatively higher transferability than genomic SSRs [84]. Recent studies showed that abundant EST-SSRs from RNA-seq have agronomic potential and constitute a scientific basis for future studies on the identification, classification, molecular verification, and innovation of germplasm in hawthorn and *Lei bamboo* [85,86].

We identified 11,338 SSRs from the annotated 61,639 unigenes. We detected 3036 mononucleotides, 5492 dinucleotides, 2493 trinucleotides, 204 tetranucleotides, 194 pentanucleotides, and 344 hexanucleotides motifs (Figure 7). Among the dinucleotide and trinucleotide SSRs, AG/CT repeats represented 2997 SSRs, and AAG/CTT repeats represented 582 SSRs. In mononucleotide, dinucleotide, trinucleotide, quadnucleotide, pentanucleotide, and hexanucleotide repeat categories, the occurrences of repeats were twelve, six, five, five, four, and four, respectively (Table S4). Finally, 6773 oligonucleotide pairs were generated for these identified SSR markers. SSRs and SNPs are the most useful and robust molecular markers for genetics and plant breeding applications [87]. This study provided a set of SSR markers that could be used, for example, in diversity analysis of *Paulownia* species. In addition, *Paulownia* tree breeding programs will benefit from the availability of these SSR markers identified from our RNAseq data. Mononucleotide SSRs would be excluded because of the frequent homopolymer errors found in sequencing data and fewer polymorphisms; dinucleotides (46.6%) and trinucleotides (21.2%) contributed most in *Paulownia*. This is consistent with the EST-SSRs distributions reported in other plant species [88,89]. In plants, SNPs are predominantly beneficial in the construction of high-resolution genetic maps, positional cloning, marker-assisted selection (MAS) of important genes, genome-wide linkage disequilibrium associate analysis, and species origin, relationship, and evolutionary studies [90].

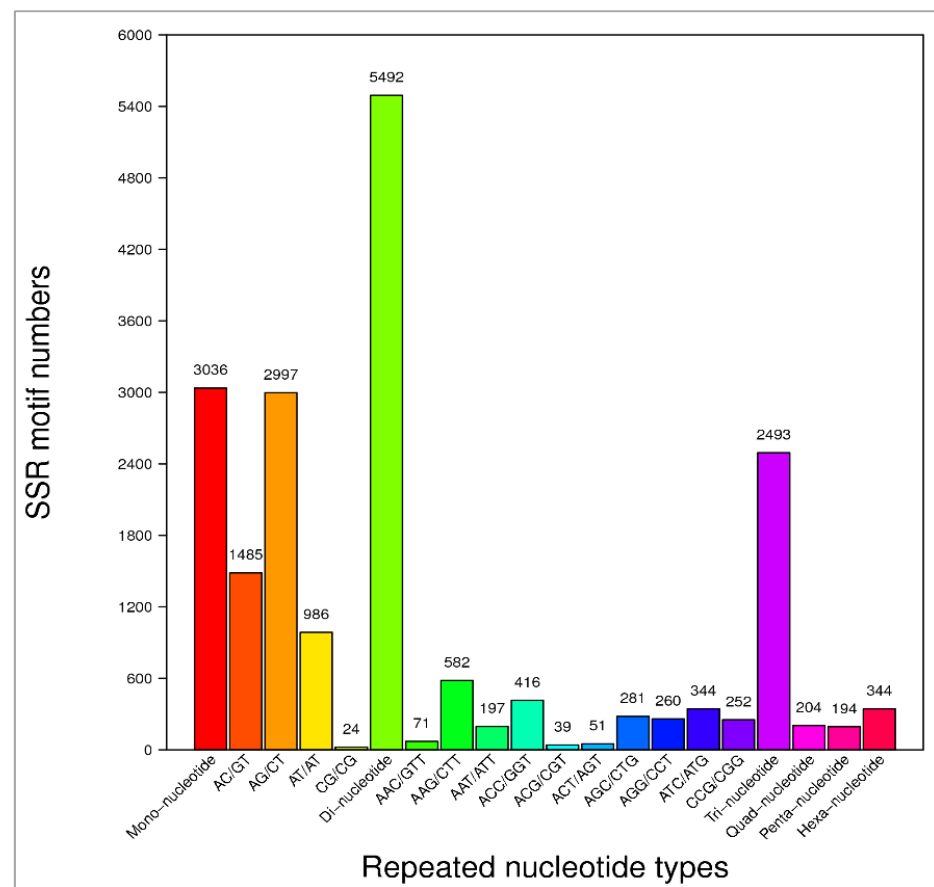


**Figure 7.** Simple sequence repeat (SSR) marker variation statistics. Number of motifs are given against each repeated nucleotide category from mono-nucleotides to hexa-nucleotides.

#### 4. Conclusions

Paulownia is a fast-growing, multipurpose timber tree suitable for use as a dedicated lignocellulosic bioenergy crop. To understand the genes involved in the formation of woody biomass related to seasonal cues, a de novo transcriptome study was conducted on vascular cambium tissue from senescent winter vascular cambium tissue and actively growing spring vascular cambium tissue. To the best of our knowledge, this is the first transcriptome-based study on *P. elongata*, as well as the first transcriptome study performed on Paulownia vascular cambium tissue focusing on seasonal difference. A set of transcripts was specifically expressed in the same set of tissues at two different time points. The transcript abundance data confirms the differential pattern of expression of cellulosic, hemicellulosic, lignin biosynthesis specific, and hormone pathway-specific genes. By analyzing the transcriptome from two different temporal treatments (winter and spring), representing two distinct physiological states of the plant, DEGs were identified from both treatments. Cell division is one of the key processes taking place in the cambial zone, and the majority of the cell cycle genes were upregulated during the active stage. The onset of cambial activity began between the end of March and the beginning of April as the increased vacuolization of meristematic cells, and the mitotic activity occurs. However, our current study showed that more genes were downregulated in the spring season. Overall, data from this study will serve as a benchmark for further analysis of molecular mechanisms of wood formation in Paulownia and other trees.

**Supplementary Materials:** The following are available online at <https://www.mdpi.com/article/10.3390/d13090423/s1>, Figure S1. Length distribution of all Paulownia unigenes, Figure S2. Statistics of differentially expressed genes, Figure S3. Unigenes involved in starch and sucrose metabolism, Figure S4. Unigenes involved in H-, G-, S-lignin biosynthesis pathway, Figure S5. Unigenes involved

in auxin biosynthesis pathway, Figure S6. Unigenes involved in cytokinin biosynthesis pathway, Table S1 Annotation BLASTX hits of unigenes in Nr database, Table S2 GO categories of unigenes, Table S3 COG function classification of unigenes, Table S4 KEGG annotation of unigenes.

**Author Contributions:** Conceptualization, N.J.; data curation, T.S.; formal analysis, A.A.; funding acquisition, N.J.; investigation, Z.D.P., C.B. and U.K.R.; methodology, Z.D.P., T.S., B.N.V. and U.K.R.; project administration, B.N.V.; validation, U.K.R.; writing—original draft, Z.D.P. and T.S.; writing—review & editing, A.A. and N.J. All authors have read and agreed to the published version of the manuscript.

**Funding:** Capacity building USDA NIFA grant ‘Developing a sustainable bioenergy system: Paulownia production for fuel, chemicals, and materials’ CSREES Award #2014-01293 (P.I: N. Joshee).

**Institutional Review Board Statement:** Not applicable.

**Informed Consent Statement:** Not applicable.

**Data Availability Statement:** Data is contained within the article or supplementary material.

**Acknowledgments:** ZP received financial assistance in the form of a graduate research assistantship (GRA) through the capacity building USDA NIFA grant ‘Developing a sustainable bioenergy system: Paulownia production for fuel, chemicals, and materials’ CSREES Award #2014-01293 (P.I: N. Joshee).

**Conflicts of Interest:** Authors declare that no competing interests exist.

## References

- Zhu, Z.-H.; Chao, C.-J.; Lu, X.-Y.; Xiong, Y.G. *Paulownia in China: Cultivation and Utilization*; Asian Network for Biological Sciences and International Development Research Centre and International Development Research Centre: Ottawa, ON, Canada, 1986; pp. 1–65.
- Clatterbuck, K.W.; Hodges, D.G. *Tree Crops for Marginal Farmland-Paulownia*; The University of Tennessee Extension Service: Knoxville, TN, USA, 2004; pp. 1–32. Available online: [https://trace.tennessee.edu/cgi/viewcontent.cgi?article=1002&context=utk\\_agexfores](https://trace.tennessee.edu/cgi/viewcontent.cgi?article=1002&context=utk_agexfores) (accessed on 26 May 2021).
- El-Showk, S.; El-Showk, N. The Paulownia Tree. An Alternative for Sustainable Forestry. 2003. Available online: [www.cropdevelopment.org](http://www.cropdevelopment.org) (accessed on 30 August 2021).
- Akyildiz, M.H.; Kol Sahin, H. Some technological properties and uses of paulownia (*Paulownia tomentosa* Steud.) wood. *J. Environ. Biol.* **2010**, *31*, 351–355.
- Li, P.; Oda, J. Flame retardancy of paulownia wood and its mechanism. *J. Mater. Sci.* **2007**, *42*, 8544–8550. [[CrossRef](#)]
- Yadav, N.K.; Vaidya, B.N.; Henderson, K.; Lee, J.F.; Stewart, W.M.; Dhekney, S.A.; Joshee, N. A Review of *Paulownia* biotechnology: A short rotation, fast growing multipurpose bioenergy tree. *Am. J. Plant. Sci.* **2013**, *4*, 2070–2082. [[CrossRef](#)]
- Tisserat, B.; Joshee, N.; Mahapatra, A.K.; Selling, G.W.; Finkenstadt, V. Physical and mechanical properties of extruded poly(lactic acid)-based *Paulownia elongata* biocomposites. *Ind. Crop. Prod.* **2013**, *44*, 88–96. [[CrossRef](#)]
- Tisserat, B.; Reifschneider, L.; Joshee, N.; Finkenstadt, V. Properties of high density polyethylene—*Paulownia* wood flour composites via injection molding. *Bioresources* **2013**, *8*, 4440–4458. [[CrossRef](#)]
- Tisserat, B.; Reifschneider, L.; Joshee, N.; Finkenstadt, V. Evaluation of *Paulownia elongata* wood polyethylene composites. *J. Thermoplast. Compos. Mater.* **2015**, *28*, 1301–1320. [[CrossRef](#)]
- Vaughn, S.F.; Dinelli, F.D.; Tisserat, B.; Joshee, N.; Vaughan, M.M.; Peterson, S.C. Creeping bentgrass growth in sand-based root zones with or without biochar. *Sci. Hortic.* **2015**, *197*, 592–596. [[CrossRef](#)]
- Stewart, W.M.; Vaidya, B.N.; Mahapatra, A.K.; Terrill, T.H.; Joshee, N. Potential use of multipurpose paulownia *elongata* tree as an animal feed resource. *Am. J. Plant. Sci.* **2018**, *9*, 1212–1227. [[CrossRef](#)]
- Ye, Z.-H.; Zhong, R. Molecular control of wood formation in trees. *J. Exp. Bot.* **2015**, *66*, 4119–4131. [[CrossRef](#)]
- Samuels, A.L.; Kaneda, M.; Rensing, K. The cell biology of wood formation: From cambial divisions to mature secondary xylem. *Can. J. Bot.* **2006**, *84*, 631–639. [[CrossRef](#)]
- Song, J.; Lu, S.; Chen, Z.-Z.; Lourenco, R.; Chiang, V.L. Genetic transformation of *populus trichocarpa* genotype nisqually-1: A functional genomic tool for woody plants. *Plant. Cell Physiol.* **2006**, *47*, 1582–1589. [[CrossRef](#)]
- Shim, D.; Ko, J.-H.; Kim, W.-C.; Wang, Q.; Keathley, D.E.; Han, K.-H. A molecular framework for seasonal growth-dormancy regulation in perennial plants. *Hortic. Res.* **2014**, *1*, 14059. [[CrossRef](#)]
- Joshee, N. Paulownia: A multipurpose tree for rapid lignocellulosic biomass production. In *Handbook of Bioenergy Crop Plants*; Kole, C., Joshi, C.P., Shonnard, D., Eds.; Taylor & Francis: Boca Raton, FL, USA, 2012; pp. 671–686.
- Aspeborg, H.; Schrader, J.; Coutinho, P.M.; Stam, M.; Kallas, A.; Djerbi, S.; Nilsson, P.; Denman, S.; Amini, B.; Sterky, F.; et al. Carbohydrate-active enzymes involved in the secondary cell wall biogenesis in hybrid aspen. *Plant. Physiol.* **2005**, *137*, 983–997. [[CrossRef](#)]
- Dharmawardhana, P.; Brunner, A.M.; Strauss, S.H. Genome-wide transcriptome analysis of the transition from primary to secondary stem development in *Populus trichocarpa*. *BMC Genom.* **2010**, *11*, 150. [[CrossRef](#)]

19. Pavy, N.; Boyle, B.; Nelson, C.; Paule, C.; Giguère, I.; Caron, S.; Parsons, L.; Dallaire, N.; Bedon, F.; Bérubé, H.; et al. Identification of conserved core xylem gene sets: Conifer cDNA microarray development, transcript profiling and computational analyses. *New Phytol.* **2008**, *180*, 766–786. [[CrossRef](#)]
20. Wang, M.; Qi, X.; Zhao, S.; Zhang, S.; Lu, M.-Z. Dynamic changes in transcripts during regeneration of the secondary vascular system in *Populus tomentosa* Carr. revealed by cDNA microarrays. *BMC Genom.* **2009**, *10*, 215. [[CrossRef](#)]
21. Wilkins, O.; Nahal, H.; Foong, J.; Provart, N.J.; Campbell, M.M. Expansion and diversification of the populus R2R3-MYB family of transcription factors. *Plant Physiol.* **2009**, *149*, 981–993. [[CrossRef](#)]
22. Dong, Y.; Fan, G.; Zhao, Z.; Deng, M. Compatible solute, transporter protein, transcription factor, and hormone-related gene expression provides an indicator of drought stress in *Paulownia fortunei*. *Funct. Integr. Genom.* **2014**, *14*, 479–491. [[CrossRef](#)]
23. Dong, Y.; Fan, G.; Zhao, Z.; Deng, M. Transcriptome expression profiling in response to drought stress in *paulownia australis*. *Int. J. Mol. Sci.* **2014**, *15*, 4583–4607. [[CrossRef](#)]
24. Mou, H.-Q.; Lu, J.; Zhu, S.-F.; Lin, C.-L.; Tian, G.-Z.; Xu, X.; Zhao, W.-J. Transcriptomic analysis of paulownia infected by paulownia witches'-broom phytoplasma. *PLoS ONE* **2013**, *8*, e77217. [[CrossRef](#)]
25. Li, B.; Zhai, X.; Cao, Y.; Zhao, H.; Wang, Z.; Liu, H.; Fan, G. Transcriptome and small RNA sequencing analysis revealed roles of PaWB-related miRNAs and genes in *Paulownia fortunei*. *Forests* **2018**, *9*, 397. [[CrossRef](#)]
26. Nitsch, J. Photoperiodism in woody plants. *J. Am. Soc. Hort. Sci.* **1957**, *70*, 526–544.
27. Espinosa-Ruiz, A.; Saxena, S.; Schmidt, J.; Mellerowicz, E.; Miskolczi, P.; Bakó, L.; Bhalerao, R.P. Differential stage-specific regulation of cyclin-dependent kinases during cambial dormancy in hybrid aspen. *Plant. J.* **2004**, *38*, 603–615. [[CrossRef](#)]
28. Wang, J.; Wang, H.; Deng, T.; Liu, Z.; Wang, X. Time-coursed transcriptome analysis identifies key expressional regulation in growth cessation and dormancy induced by short days in *Paulownia*. *Sci. Rep.* **2019**, *9*, 16602. [[CrossRef](#)]
29. Immanen, J.; Nieminen, K.; Smolander, O.-P.; Kojima, M.; Serra, J.A.; Koskinen, P.; Zhang, J.; Elo, A.; Mähönen, A.P.; Street, N. Cytokinin and auxin display distinct but interconnected distribution and signaling profiles to stimulate cambial activity. *Curr. Biol.* **2016**, *26*, 1990–1997. [[CrossRef](#)]
30. Nieminen, K.; Blomster, T.; Helariutta, Y.; Mähönen, A.P. Vascular cambium development. *Arab. Book* **2015**, *13*, e0177. [[CrossRef](#)]
31. Qiu, Z.; He, Y.; Zhang, Y.; Guo, J.; Zhang, L. Genome-wide identification and profiling of microRNAs in *Paulownia tomentosa* cambial tissues in response to seasonal changes. *Gene* **2018**, *677*, 32–40. [[CrossRef](#)]
32. Saminathan, T.; Nimmakayala, P.; Manohar, S.; Malkaram, S.; Almeida, A.; Cantrell, R.; Tomason, Y.; Abburi, L.; Rahman, M.A.; Vajja, V.G.; et al. Differential gene expression and alternative splicing between diploid and tetraploid watermelon. *J. Exp. Bot.* **2015**, *66*, 1369–1385. [[CrossRef](#)]
33. Grabherr, M.G.; Haas, B.J.; Yassour, M.; Levin, J.; Thompson, D.A.; Amit, I.; Adiconis, X.; Fan, L.; Raychowdhury, R.; Zeng, Q.; et al. Full-length transcriptome assembly from RNA-Seq data without a reference genome. *Nat. Biotechnol.* **2011**, *29*, 644–652. [[CrossRef](#)]
34. Kanehisa, M.; Araki, M.; Goto, S.; Hattori, M.; Hirakawa, M.; Itoh, M.; Katayama, T.; Kawashima, S.; Okuda, S.; Tokimatsu, T.; et al. KEGG for linking genomes to life and the environment. *Nucleic Acids Res.* **2007**, *36*, D480–D484. [[CrossRef](#)]
35. Conesa, A.; Götz, S.; García-Gómez, J.M.; Terol, J.; Talón, M.; Robles, M. Blast2GO: A universal tool for annotation, visualization and analysis in functional genomics research. *Bioinformatics* **2005**, *21*, 3674–3676. [[CrossRef](#)]
36. Iseli, C.; Jongeneel, C.V.; Bucher, P. ESTScan: A program for detecting, evaluating, and reconstructing potential coding regions in EST sequences. *Proc. Int. Conf. Intell. Syst. Mol. Biol.* **1999**, *99*, 138–148.
37. Langmead, B.; Salzberg, S.L. Fast gapped-read alignment with Bowtie. *Nat. Methods* **2012**, *9*, 357–359. [[CrossRef](#)]
38. Li, B.; Dewey, C.N. RSEM: Accurate transcript quantification from RNA-Seq data with or without a reference genome. *BMC Bioinform.* **2011**, *12*, 323. [[CrossRef](#)]
39. Tarazona, S.; García-Alcalde, F.; Dopazo, J.; Ferrer, A.; Conesa, A. Differential expression in RNA-seq: A matter of depth. *Genome Res.* **2011**, *21*, 2213–2223. [[CrossRef](#)]
40. Doering, A.; Lathe, R.; Persson, S. An Update on xylan synthesis. *Mol. Plant.* **2012**, *5*, 769–771. [[CrossRef](#)]
41. Jia, X.-L.; Wang, G.-L.; Xiong, F.; Yu, X.-R.; Xu, Z.-S.; Wang, F.; Xiong, A.-S. De novo assembly, transcriptome characterization, lignin accumulation and anatomic characteristics: Novel insights into lignin biosynthesis during celery leaf development. *Sci. Rep.* **2015**, *5*, srep08259. [[CrossRef](#)]
42. Pauly, M.; Gille, S.; Liu, L.; Mansoori, N.; de Souza, A.J.; Schultink, A.; Xiong, G. Hemicellulose biosynthesis. *Planta* **2013**, *238*, 627–642. [[CrossRef](#)]
43. Quang, T.H.; Hallingback, H.R.; Gyllenstrand, N.; Von Arnold, S.; Clapham, D. Expression of genes of cellulose and lignin synthesis in *Eucalyptus urophylla* and its relation to some economic traits. *Trees* **2011**, *26*, 893–901. [[CrossRef](#)]
44. Livak, K.J.; Schmittgen, T.D. Analysis of relative gene expression data using real-time quantitative PCR and the  $2^{-\Delta\Delta CT}$  method. *Methods* **2001**, *25*, 402–408. [[CrossRef](#)]
45. Novaes, E.; Drost, D.R.; Farmerie, W.G.; Pappas, G.J.; Grattapaglia, D.; Sederoff, R.R.; Kirst, M. High-throughput gene and SNP discovery in *Eucalyptus grandis*, an uncharacterized genome. *BMC Genom.* **2008**, *9*, 312. [[CrossRef](#)]
46. Wang, C.; Wang, Y.; Diao, G.; Jiang, J.; Yang, C. Isolation and characterization of expressed sequence tags (ESTs) from cambium tissue of birch (*Betula platyphylla* Suk). *Plant. Mol. Biol. Rep.* **2010**, *28*, 438–449. [[CrossRef](#)]
47. Xu, E.; Fan, G.; Niu, S.; Zhao, Z.; Deng, M.; Dong, Y. Transcriptome-wide profiling and expression analysis of diploid and autotetraploid paulownia *tomentosa* × paulownia *fortunei* under drought stress. *PLoS ONE* **2014**, *9*, e113313. [[CrossRef](#)]

48. Zhao, H.; Li, R.; Shang, F. The complete chloroplast genome of *Paulownia elongata* and phylogenetic implications in Lamiales. *Mitochondrial DNA Part B* **2019**, *4*, 2067–2068. [[CrossRef](#)]
49. Zhu, Y.; Song, D.; Sun, J.; Wang, X.; Li, L. PtrHB7, a class III HD-zip gene, plays a critical role in regulation of vascular cambium differentiation in populus. *Mol. Plant.* **2013**, *6*, 1331–1343. [[CrossRef](#)]
50. Groover, A.T.; Mansfield, S.D.; DiFazio, S.; Dupper, G.; Fontana, J.R.; Millar, R.; Wang, Y. The populus homeobox gene ARBORKNOX1 reveals overlapping mechanisms regulating the shoot apical meristem and the vascular cambium. *Plant. Mol. Biol.* **2006**, *61*, 917–932. [[CrossRef](#)]
51. Li, E.; Bhargava, A.; Qiang, W.; Friedmann, M.C.; Forneris, N.; Savidge, R.A.; Johnson, L.A.; Mansfield, S.; Ellis, B.E.; Douglas, C.J. The class II KNOX gene KNAT7 negatively regulates secondary wall formation in Arabidopsis and is functionally conserved in Populus. *New Phytol.* **2012**, *194*, 102–115. [[CrossRef](#)]
52. Pines, J. Cubism and the cell cycle: The many faces of the APC/C. *Nat. Rev. Mol. Cell Biol.* **2011**, *12*, 427–438. [[CrossRef](#)]
53. Hertzberg, M.; Aspeborg, H.; Schrader, J.; Andersson, A.; Erlandsson, R.; Blomqvist, K.; Bhalerao, R.; Uhlen, M.; Teeri, T.T.; Lundeberg, J.; et al. A transcriptional roadmap to wood formation. *Proc. Natl. Acad. Sci. USA* **2001**, *98*, 14732–14737. [[CrossRef](#)]
54. Hu, Z.; Liu, Q.; Tan, M.; Yi, H.; Deng, X. Lignin deposition converts juice sacs to “Brown Thorns” in a citrus triploid hybrid. *J. Am. Soc. Hortic. Sci.* **2008**, *133*, 173–177. [[CrossRef](#)]
55. Jokipii-Lukkari, S.; Delhomme, N.; Schiffthaler, B.; Mannapperuma, C.; Prestele, J.; Nilsson, O.; Street, N.R.; Tuominen, H. Transcriptional roadmap to seasonal variation in wood formation of norway spruce. *Plant. Physiol.* **2018**, *176*, 2851–2870. [[CrossRef](#)]
56. Mauseth, J.D. *Plant Anatomy*; The Benjamin/Cummings: San Francisco, CA, USA, 1988; p. 560.
57. Zhong, R.; Ye, Z.-H. Secondary cell walls: Biosynthesis, patterned deposition and transcriptional regulation. *Plant. Cell Physiol.* **2015**, *56*, 195–214. [[CrossRef](#)]
58. Villalobos, D.P.; Moreno, R.B.; Said, E.-S.S.; Cañas, R.A.; Osuna, D.; Van Kerckhoven, S.H.E.; Bautista, R.; Claros, M.G.; Canovas, F.M.; Cantón, F.R. Reprogramming of gene expression during compression wood formation in pine: Coordinated modulation of S-adenosylmethionine, lignin and lignan related genes. *BMC Plant. Biol.* **2012**, *12*, 100. [[CrossRef](#)]
59. Turcotte, A.; Morin, H.; Krause, C.; Deslauriers, A.; Thibeault-Martel, M. The timing of spring rehydration and its relation with the onset of wood formation in black spruce. *Agric. For. Meteorol.* **2009**, *149*, 1403–1409. [[CrossRef](#)]
60. Djerbi, S.; Aspeborg, H.; Nilsson, P.; Sundberg, B.; Mellerowicz, E.; Blomqvist, K.; Teeri, T.T. Identification and expression analysis of genes encoding putative cellulose synthases (CesA) in the hybrid aspen, *Populus tremula* (L.) *P. tremuloides* (Michx.). *Cellulose* **2004**, *11*, 301–312. [[CrossRef](#)]
61. Davis, J.; Brandizzi, F.; Liepman, A.H.; Keegstra, K. Arabidopsis mannan synthase CSLA9 and glucan synthase CSLC4 have opposite orientations in the Golgi membrane. *Plant. J.* **2010**, *64*, 1028–1037. [[CrossRef](#)]
62. Perrin, R.M.; DeRocher, A.E.; Bar-Peled, M.; Zeng, W.; Norambuena, L.; Orellana, A.; Raikhel, N.V.; Keegstra, K. Xyloglucan fucosyltransferase, an enzyme involved in plant cell wall biosynthesis. *Science* **1999**, *284*, 1976–1979. [[CrossRef](#)] [[PubMed](#)]
63. Vanzin, G.; Madson, M.; Carpita, N.C.; Raikhel, N.V.; Keegstra, K.; Reiter, W.-D. The mur2 mutant of Arabidopsis thaliana lacks fucosylated xyloglucan because of a lesion in fucosyltransferase AtFUT. *Proc. Natl. Acad. Sci. USA* **2002**, *99*, 3340–3345. [[CrossRef](#)]
64. Gille, S.; de Souza, A.J.; Xiong, G.; Benz, M.; Cheng, K.; Schultink, A.; Reca, I.-B.; Pauly, M. O-Acetylation of arabidopsis hemicellulose xyloglucan requires AX4 or AX4L, proteins with a TBL and DUF231 domain. *Plant. Cell* **2011**, *23*, 4041–4053. [[CrossRef](#)]
65. Kong, Y.; Zhou, G.; Avci, U.; Gu, X.; Jones, C.; Yin, Y.; Xu, Y.; Hahn, M. Two poplar glycosyltransferase genes, PdGATL1.1 and PdGATL1.2, are functional orthologs to PARVUS/AtGATL1 in arabidopsis. *Mol. Plant.* **2009**, *2*, 1040–1050. [[CrossRef](#)]
66. Hörnblad, E.; Ulfstedt, M.; Ronne, H.; Marchant, A. Partial functional conservation of IRX10 homologs in physcomitrella patens and Arabidopsis thaliana indicates an evolutionary step contributing to vascular formation in land plants. *BMC Plant. Biol.* **2013**, *13*, 3. [[CrossRef](#)] [[PubMed](#)]
67. Lefebvre, V.; Fortabat, M.-N.; Ducamp, A.; North, H.M.; Maia-Grondard, A.; Trouverie, J.; Boursiac, Y.; Mouille, G.; Durand-Tardif, M. ESKIMO1 disruption in arabidopsis alters vascular tissue and impairs water transport. *PLoS ONE* **2011**, *6*, e16645. [[CrossRef](#)]
68. Hu, W.-J.; Harding, S.A.; Lung, J.; Popko, J.L.; Ralph, J.; Stokke, D.D.; Tsai, C.-J.; Chiang, V.L. Repression of lignin biosynthesis promotes cellulose accumulation and growth in transgenic trees. *Nat. Biotechnol.* **1999**, *17*, 808–812. [[CrossRef](#)]
69. Goujon, T.; Ferret, V.; Mila, I.; Pollet, B.; Ruel, K.; Burlat, V.; Joseleau, J.-P.; Barrière, Y.; Lapierre, C.; Jouanin, L. Down-regulation of the AtCCR1 gene in Arabidopsis thaliana: Effects on phenotype, lignins and cell wall degradability. *Planta* **2003**, *217*, 218–228. [[CrossRef](#)]
70. Bouvier d’Yvoire, M.; Bouchabke-Coussa, O.; Voorend, W.; Antelme, S.; Cézard, L.; Legée, F.; Lebris, P.; Legay, S.; Whitehead, C.; McQueen-Mason, S.J. Disrupting the cinnamyl alcohol dehydrogenase 1 gene (Bd CAD 1) leads to altered lignification and improved saccharification in Brachypodium distachyon. *Plant J.* **2013**, *73*, 496–508. [[CrossRef](#)]
71. Stepanova, A.; Robertson-Hoyt, J.; Yun, J.; Benavente, L.M.; Xie, D.-Y.; Dolezal, K.; Schlereth, A.; Jürgens, G.; Alonso, J.M. TAA1-mediated auxin biosynthesis is essential for hormone crosstalk and plant development. *Cell* **2008**, *133*, 177–191. [[CrossRef](#)]
72. Cheng, Y.; Dai, X.; Zhao, Y. Auxin biosynthesis by the YUCCA flavin monooxygenases controls the formation of floral organs and vascular tissues in Arabidopsis. *Genes Dev.* **2006**, *20*, 1790–1799. [[CrossRef](#)]

73. Won, C.; Shen, X.; Mashiguchi, K.; Zheng, Z.; Dai, X.; Cheng, Y.; Kasahara, H.; Kamiya, Y.; Chory, J.; Zhao, Y. Conversion of tryptophan to indole-3-acetic acid by tryptophan aminotransferases of arabidopsis and yuccas in arabidopsis. *Proc. Natl. Acad. Sci. USA* **2011**, *108*, 18518–18523. [[CrossRef](#)]
74. Hu, H.; Zhang, R.; Feng, S.; Wang, Y.; Wang, Y.; Fan, C.; Li, Y.; Liu, Z.; Schneider, R.; Xia, T. Three AtCesA6-like members enhance biomass production by distinctively promoting cell growth in Arabidopsis. *Plant Biotechnol. J.* **2018**, *16*, 976–988. [[CrossRef](#)]
75. Liners, F.; Gaspar, T.; Van Cutsem, P. Acetyl- and methyl-esterification of pectins of friable and compact sugar-beet calli: Consequences for intercellular adhesion. *Planta* **1994**, *192*, 545–556. [[CrossRef](#)]
76. Turner, S.R.; Somerville, C.R. Collapsed xylem phenotype of Arabidopsis identifies mutants deficient in cellulose deposition in the secondary cell wall. *Plant. Cell* **1997**, *9*, 689–701. [[CrossRef](#)] [[PubMed](#)]
77. Sundberg, B.; Uggla, C.; Tuominen, H.; Savidge, R.; Barnett, J.; Napier, R. *Cell and Molecular Biology of Wood Formation*; BIOS Scientific Publishers: Oxford, UK; pp. 169–188.
78. Savidge, R.A. The role of plant hormones in higher plant cellular differentiation. II. Experiments with the vascular cambium, and sclereid and tracheid differentiation in the pine, *Pinus contorta*. *J. Mol. Histol.* **1983**, *15*, 447–466. [[CrossRef](#)] [[PubMed](#)]
79. Matsumoto-Kitano, M.; Kusumoto, T.; Tarkowski, P.; Kinoshita-Tsujimura, K.; Václavíková, K.; Miyawaki, K.; Kakimoto, T. Cytokinins are central regulators of cambial activity. *Proc. Natl. Acad. Sci. USA* **2008**, *105*, 20027–20031. [[CrossRef](#)]
80. Bevan, M.; Northcote, D.H. The interaction of auxin and cytokinin in the induction of phenylalanine ammonia-lyase in suspension cultures of *Phaseolus vulgaris*. *Planta* **1979**, *147*, 77–81. [[CrossRef](#)]
81. Stepanova, A.; Yun, J.; Robles, L.M.; Novak, O.; He, W.; Guo, H.; Ljung, K.; Alonso, J.M. The arabidopsis YUCCA1 flavin monooxygenase functions in the indole-3-pyruvic acid branch of auxin biosynthesis. *Plant. Cell* **2011**, *23*, 3961–3973. [[CrossRef](#)] [[PubMed](#)]
82. Barbará, T.; Palma-Silva, C.; Paggi, G.; Bered, F.; Fay, M.F.; Lexer, C. Cross-species transfer of nuclear microsatellite markers: Potential and limitations. *Mol. Ecol.* **2007**, *16*, 3759–3767. [[CrossRef](#)]
83. Powell, W.; Machray, G.C.; Provan, J. Polymorphism revealed by simple sequence repeats. *Trends Plant Sci.* **1996**, *1*, 215–222. [[CrossRef](#)]
84. Varshney, R.; Graner, A.; Sorrells, M.E. Genic microsatellite markers in plants: Features and applications. *Trends Biotechnol.* **2005**, *23*, 48–55. [[CrossRef](#)] [[PubMed](#)]
85. Cai, K.; Zhu, L.; Zhang, K.; Li, L.; Zhao, Z.; Zeng, W.; Lin, X. Development and characterization of EST-SSR markers from RNA-seq data in *Phyllostachys violascens*. *Front. Plant. Sci.* **2019**, *10*, 50. [[CrossRef](#)] [[PubMed](#)]
86. Ma, S.; Dong, W.; Lyu, T.; Lyu, Y. An RNA sequencing transcriptome analysis and development of EST-SSR markers in chinese hawthorn through illumina sequencing. *Forest* **2019**, *10*, 82. [[CrossRef](#)]
87. Hiremath, P.J.; Kumar, A.; Penmetsa, R.V.; Farmer, A.; Schlueter, J.; Chamarthi, S.K.; Whaley, A.M.; Carrasquilla-Garcia, N.; Gaur, P.; Upadhyaya, H.D.; et al. Large-scale development of cost-effective SNP marker assays for diversity assessment and genetic mapping in chickpea and comparative mapping in legumes. *Plant. Biotechnol. J.* **2012**, *10*, 716–732. [[CrossRef](#)]
88. Ahn, Y.-K.; Tripathi, S.; Cho, Y.-I.; Kim, J.-H.; Lee, H.-E.; Kim, D.-S.; Woo, J.-G.; Cho, M.-C. De novo transcriptome assembly and novel microsatellite marker information in *Capsicum annuum* varieties Saengryeg 211 and Saengryeg 213. *Bot. Stud.* **2013**, *54*, 58. [[CrossRef](#)]
89. Wang, Z.; Yu, G.; Shi, B.; Wang, X.; Qiang, H.; Gao, H. Development and characterization of simple sequence repeat (SSR) markers based on RNA-sequencing of *Medicago sativa* and in silico mapping onto the *M. truncatula* genome. *PLoS ONE* **2014**, *9*, e92029. [[CrossRef](#)] [[PubMed](#)]
90. Shahinnia, F.; Sayed-Tabatabaei, B.E. Conversion of barley SNPs into PCR-based markers using dCAPS method. *Genet. Mol. Biol.* **2009**, *32*, 564–567. [[CrossRef](#)]